JETS IN POLAR CORONAL HOLES

E. Scullion[1], M. D. Popescu[1], D. Banerjee[2], J. G. Doyle[1], AND R. Erdélyi[3]

[1] Armagh Observatory, College Hill, Armagh BT61 9DG, UK; ems@arm.ac.uk, mdp@arm.ac.uk, jgd@arm.ac.uk
[2] Indian Institute of Astrophysics, Koramangala, Bangalore 560034, India; dipu@iiap.res.in
[3] Solar Physics and Space Plasma Research Centre (SP2RC), Department of Applied Mathematics, University of Sheffield,
Sheffield S3 7RH, UK; robertus@sheffield.ac.uk
Received 2009 May 17; accepted 2009 September 11; published 2009 October 1

ABSTRACT

Here, we explore the nature of small-scale jet-like structures and their possible relation to explosive events and other known transient features, like spicules and macrospicules, using high-resolution spectroscopy obtained with the *Solar and Heliospheric Observatory*/Solar Ultraviolet Measurements of Emitted Radiation instrument. We present a highly resolved spectroscopic analysis and line parameter study of time-series data for jets occurring on-disk and off-limb in both a northern and a southern coronal hole. The analysis reveals many small-scale transients which rapidly propagate between the mid-transition region (N IV 765 Å line formation: 140,000 K) and the lower corona (Ne VIII 770 Å line formation: 630,000 K). In one example, a strong jet-like event is associated with a cool feature not present in the Ne VIII 770 Å line radiance or Doppler velocity maps. Another similar event is observed, but with a hot component, which could be perceived as a blinker. Our data reveal fast, repetitive plasma outflows with blueshift velocities of ≈145 km s^{-1} in the lower solar atmosphere. The data suggest a strong role for smaller jets (spicules), as a precursor to macrospicule formation, which may have a common origin with explosive events.

Key words: line: profiles – Sun: chromosphere – Sun: transition region – Sun: UV radiation – techniques: spectroscopic

Online-only material: color figures

1. INTRODUCTION

Polar coronal holes (pCHs) are regions of the outer solar atmosphere which have a predominantly open magnetic field configuration (Krieger et al. 1973). They consist of a cool and low-density plasma which appear "dark" in contrast with the million degree temperatures of the corona (Munro & Withbroe 1972). The recent launch of *Hinode* (Kosugi et al. 2007) with three onboard instruments, namely, Extreme Ultraviolet Imaging Spectrometer (EIS; Culhane et al. 2007), Solar Optical Telescope (SOT; Tsuneta et al. 2008), and X-Ray Telescope (XRT; Golub et al. 2007) has provided ubiquitous observations of many jets in pCHs as well as evidence of localized regions with very strong kG magnetic fields. *Hinode*/XRT records jets at an order of magnitude higher rate than previously thought (Cirtain et al. 2007). Consequently, jets may have a more significant impact on the solar atmosphere than previously accounted for (Savcheva et al. 2007; Chifor et al. 2008; Moreno-Insertis et al. 2008).

A variety of jet-like transient events appear in pCHs in the form of spicules, macrospicules, and surges (Beckers 1972; Sterling 2000). Spicules are thin jet-like features best observed off-limb. De Pontieu et al. (2007b) suggested two spicule types with different dynamic properties. Type-I spicules have a birth rate of 0.16 per minute (making them the most common feature in the lower to mid-solar atmosphere) with 4–10 minutes lifetimes, 1500 km widths, typical rise velocity of 25 km s^{-1} rise velocity and reach heights of 7–10 Mm above the solar surface. Type-II spicules (as revealed by *Hinode* SOT) are much more dynamic and tend to dominate the limb in pCHs (De Pontieu et al. 2007b, 2007c). They have typical lifetimes of 10–150 s, are smaller in height, and have rise velocities a factor of 2–5 times greater than Type I. Larger spicules, namely, macrospicules, are frequently observed to reach heights of 40 Mm off-limb near polar regions and can have lifetimes greater than 20 minutes

(Pike & Mason 1998; Nishizuka et al. 2009). Macrospicules, along with other pCH jets, have been proposed to originate as a result of a magnetic reconnection process which drives Alfvén waves through the atmosphere (De Pontieu et al. 2007a). It has been demonstrated that jets can be produced by magnetic reconnection between pre-existing fields and newly emerging fields (Shibata et al. 1992). It has been proposed that both types of spicule jets undergo Alfvénic motions (De Pontieu et al. 2007b). Although this finding has recently faced some scrutiny with respect to the potential misinterpretation of the transverse spicule motions as indicators of Alfvén waves rather than fast kink wave propagation (Zaqarashvili & Erdélyi 2009). Alfvénic waves may, only, be indirectly measured via a spectroscopic line width approach as carried out by Jess et al. (2009).

Off-limb spicules are found to exhibit a twisted thread structure with high-resolution imaging (Suematsu et al. 2008). Similarly, a helical structure has been observed in EUV jets (Zaqarashvili & Skhirtladze 2008) and, also, with *STEREO* using the EUVI/SECCHI instrument for polar coronal jets (Patsourakos et al. 2008). SOT can provide exceptionally high spatial resolution images of the dynamic chromosphere, yet, it has become increasingly apparent that spectroscopic observations give more valuable information regarding jet activity through variation of emission line profiles. Doppler velocity and spectral analysis is required to determine the actual plasma motions rather than the apparent motions of jets. Spectroscopic observations of Kamio et al. (2007) determined the Doppler velocities using spectra from EIS for jets which suggest a blueshift of 30 km s^{-1}. They have shown that line fitting of EIS spectral data reveals a non-Gaussian component at the location of the jet with a strongly blueshifted "wing" indicating line-of-sight velocities of 80–100 km s^{-1}. Such velocities suggest an explosive nature in the jets formation.

Spectral line fitting of EIS data can give us information on the hot coronal plasma but what is the effect lower in the
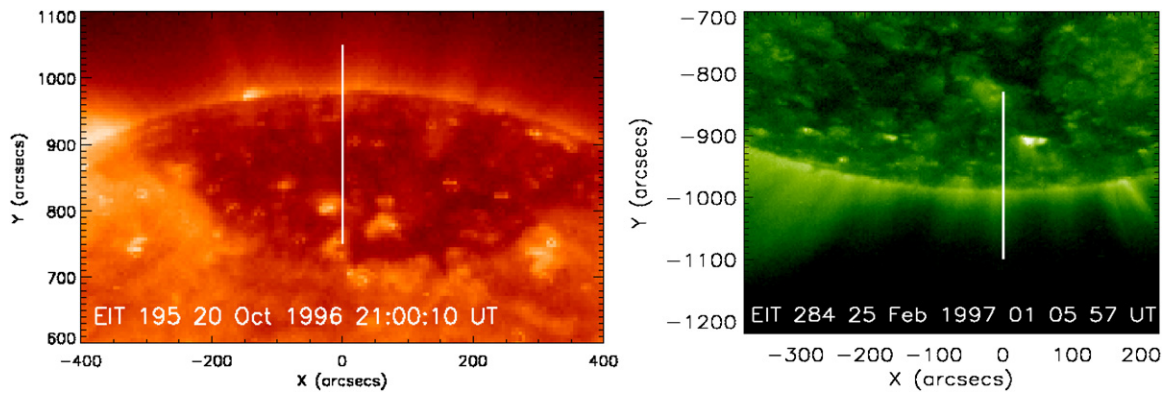
Figure 1. Location of the *SOHO*/SUMER B2 slit in the NPCH (left) and SPCH (right) for 4 hr and 8 hr "sit and stare" time-series observations superimposed on EIT 195 Å and 284 Å images.

(A color version of this figure is available in the online journal.)

Table 1
Temporal Series Observation from SUMER in Polar Coronal Holes (pCHs)

Location	North Polar Coronal Hole	South Polar Coronal Hole
Date	1996 Oct 20	1997 Feb 25
Time UT	19:57–23:57	00:03–13:58
Position (X, Y)	(0, 909.75)	(0, −950.25)
Lines	N IV 765.15 Å Ne VIII 770.42 Å	N IV 765.15 Å Ne VIII 770.42 Å
Exposure time (s)	30	60

atmosphere, e.g., the transition region and lower corona? Furthermore, a clear understanding on how limb events appear when seen on-disk still does not exist in the literature. McIntosh & De Pontieu (2009) noted several questions concerning the relationship between chromospheric spicules and the emitting transition region structures observed above the limb. In an attempt to address some of these issues, we analyze spectroscopic data taken with the *Solar and Heliospheric Observatory*/Solar Ultraviolet Measurements of Emitted Radiation (*SOHO*/SUMER) spectrograph (Wilhelm et al. 1995) in pCH regions (see Figure 1). These data give us not only line shift information but information on the excess line widths which are an important tracer of energy deposition in the solar atmosphere (Doschek et al. 2007).

2. DATA

The data analyzed here (see Table 1) were acquired with the SUMER spectrograph using slit B (1 × 300 arcsec field of view; 1 arcsec ($''$) at L1 corresponds to 715 km on the Sun's surface). The slit width ($1''$) is the spatial resolution in the *x*-direction which is the same as the spatial resolution along the *y*-direction (north–south). The spectral resolution of the instrument is 40 mÅ per pixel and we use two windows of 50 pixels each enabling accurate resolution of the two selected emission lines.

The observations consist of time-series data sets otherwise known as "sit and stare." The fixed position of the slits for the northern pCH (NPCH) and the southern pCH (SPCH) is presented on EIT 195 Å and EIT 284 Å images, respectively (see Figure 1), with part of the slit off-limb and part on-disk.

We study the variation of the emission line profiles for two lines: N IV 765.15 Å and Ne VIII 770.42 Å originating around 140,000 K (transition region) and 630,000 K (low corona), respectively. The standard reduction of SUMER raw images follows several stages, namely, decompression and reversion, dead-time correction, local gain correction, flat-field correction, a correction for geometrical distortion, and

radiometric calibration (Dammasch et al. 1999). Instrumental broadening of the spectral line profiles must be extracted in order to correctly interpret the full width at half-maximum (FWHM) line parameter. We applied a procedure first outlined by Dammasch et al. (1999), and as shown by Xia (2003) and applied in Popescu et al. (2005, 2007). These results are statistically consistent with those obtained by using a standard Gaussian fitting program.

A further correction is required after fitting of the data. This involves a correction of the returned Doppler velocity map for thermal heating of the detector and to eliminate systematic variation along the slit. During lengthy observations, this presents a periodic drift of the whole spectral image. The uncertainty in velocity from this calculation is ± 1.2 km s^{-1}.

This problem can be solved with a limb correction and a smoothing procedure. We assume that the Doppler velocity shift off-limb is net zero.

Figures 2 and 3 present the results of the fitted data. The images reveal the variations of the line parameters along the slit over the duration of the observation for N IV 765 Å and Ne VIII 770 Å of both pCHs.

3. RESULTS

In this section, we study some of the interesting features from the global maps presented in Figures 2 and 3 in more detail. As shown in Popescu et al. (2007), searching for jet-like or explosive events is greatly enabled through the use of FWHM mapping. Localized events with non-Gaussian spectral line profiles appear as bright regions in the FWHM maps.

The radiance and FWHM time-series maps are plotted logarithmically, hence, the brighter features represent significantly higher values of the two parameters. The Doppler velocity maps show line shifts in the range of ± 10 km s^{-1}. Initial analysis of the coronal hole observations reveals that there is an indication of largely blueshifted plasma in the Ne VII 770 Å emission
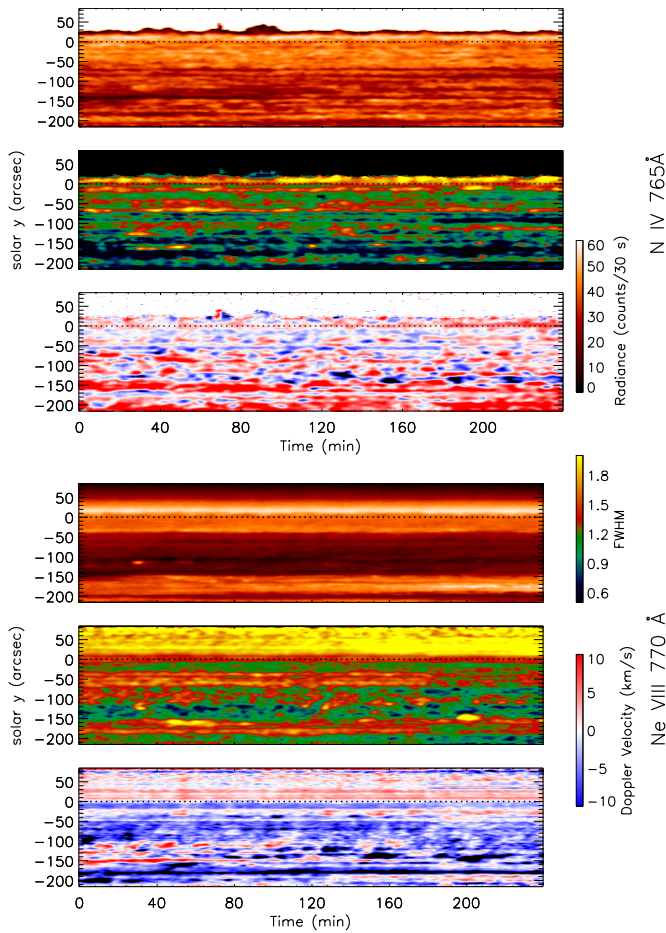
Figure 2. Time-series radiance, Doppler velocity, and line width (FWHM) maps in the N IV 765 Å (top) and Ne VIII 770 Å (bottom) as seen in the NPCH. The *x*-axis indicates the time of the observation (minutes) with 30 s time intervals per exposure. Total observation time is 240 minutes. The *y*-axis of each plot denotes the length along the slit (units of arcsec) with the origin centered on the limb position (marked with a dashed line). The positive end of the axis represents the height above the limb and vice versa for the negative values. A logarithmic color scale is used for the radiance maps to highlight any activity on the limb.

(A color version of this figure is available in the online journal.)

which corresponds with higher radiance. Ne VII 770 Å is considered to be a good tracer for the origins of plasma outflow in the fast solar wind. It is the coolest low corona/high transition region species for which we see outflow in pCHs. Largely red-shifted regions on-disk for both pCHs in the N IV 765 Å line are believed to occur because most of the spicular plasma on-disk does not escape as fast solar wind but falls back to the surface. The location of the origin along the *y*-axis indicates the limb position. The limb is found through repeating the single line fitting procedure with continuum spectral data in each pixel. A faint off-limb macrospicule event in N IV 765 Å in Figure 2 (at ≈70 minutes) and two similar events in Figure 3 (at $t ≈$ 450–500 minutes and $t ≈$ 750–800 minutes) can immediately be identified. Many tiny elongated structures (jet-like features) can be easily revealed on-disk in the velocity maps and, also, in the line width maps (particularly in Figure 3).

There is a strong indication of repetitive plasma outflow in Figure 2 between Solar $Y = -100''$ and $-150''$ in N IV 765 Å and at times $t =$ 120–140 minutes, $t =$ 150–160 minutes, $t =$ 180–190 minutes, and $t =$ 210–220 minutes. Each of these events has similar coverage along the slit ($25''$ range) and each outflow has an average line-of-sight blueshifted velocity
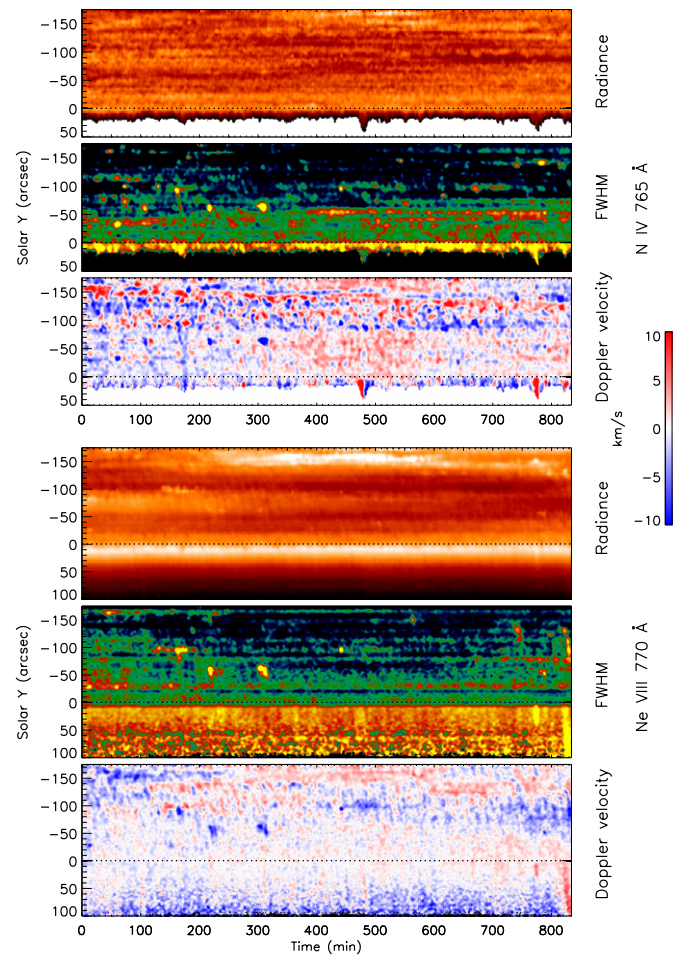
Figure 3. Time-series radiance, Doppler velocity, and line width (FWHM) maps in the N IV 765 Å (top) and Ne VIII 770 Å (bottom) as seen in the SPCH. The *x*-axis indicates the time of the observation (minutes) with 60 s time intervals per exposure. The positive end of the axis represents the height above the limb and vice versa for the negative values. Total observation time is 840 minutes.

(A color version of this figure is available in the online journal.)

of ≈25 km s^{-1}. The periodicity of these consecutive outflows corresponds to ∼20–25 minutes and each burst lasts typically 10–12 minutes. What is interesting is that these plasma outbursts seen in N IV 765 Å are, also, evident in the Ne VIII 770 Å Doppler velocity maps but with stronger outflows (greater than 25 km s^{-1}), similar spatial coverage and an overall longer duration. From the FWHM maps of both pCHs, we find many locations with very large line widths. One particular event in Figure 2 between 200–210 minutes and $-100''$ and $-150''$ exhibits stronger plasma outflow and increased line width in the hotter line than in the cooler. This FWHM activity maybe connected with the preceding repetitive outflows in the cooler line. We will discuss this feature in more detail in Section 3 for Jet 2. Figure 3 reveals substantial activity in the SPCH off-limb in N IV 765 Å along with many bright regions in both hotter and cooler FWHM maps. In the following subsections, we will focus on a number of these interesting events.

3.1. Jet 1

Figure 4 shows the temporal variation of both N IV 765 Å and Ne VIII 770 Å for a macrospicule which extends up to $40''$ off-limb in the NPCH. This jet is clearly identifiable in all three line parameter maps of N IV 765 Å and has a duration of
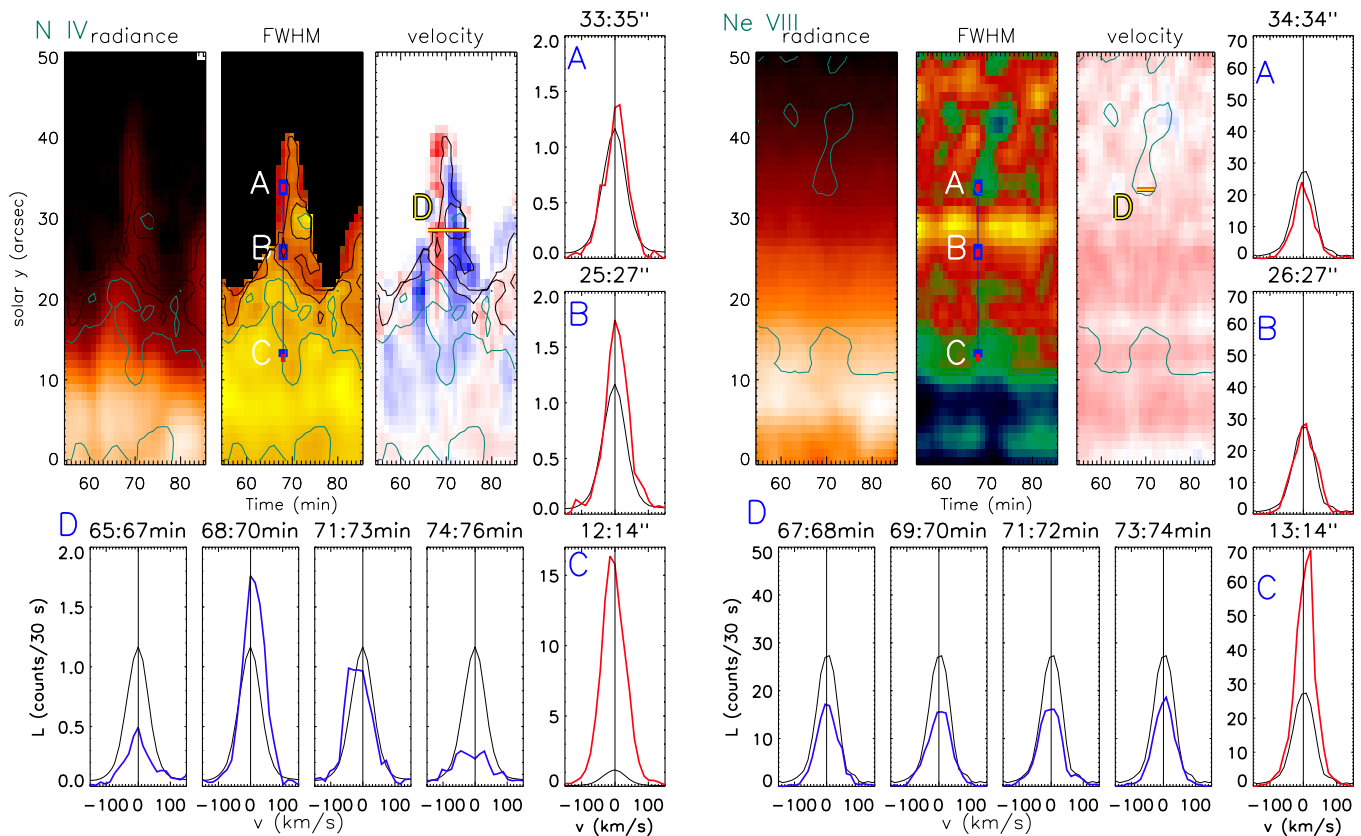
Figure 4. Time-series radiance, Doppler velocity, and width (FWHM) maps in N IV 765 Å (left) and Ne VIII 770 Å (right) for the macrospicule event off-limb in the NPCH. Surrounding each of the line parameter maps are the fitted spectral line profiles representing the locations marked on the maps by A, B, and C (red spectral lines) which describe the spatial evolution of the line at one time. Marker D (blue spectral lines) describes the temporal evolution of the line at one location along the slit. The black line profile represents the mean line profile found through summing each fitted spectral pixel window between 10″ and 40″ off-limb for the full duration of the observation. The contours on all maps are those of the FWHM data of both lines, respectively, with values of 1.4 spectral pixels (light) and 1.6 spectral pixels (dark).

(A color version of this figure is available in the online journal.)

15–20 minutes. It is not visible in Ne VIII 770 Å possibly because of insufficient heating or low density at higher temperatures. In N IV 765 Å at ≈63 minutes, there is a jet which reaches a height of ≈24″ within 2 minutes and lasts for ≈5 minutes. This corresponds to a strong blueshift. This jet enters a second stage in which the plasma at ∼27″ off-limb appears to accelerate to ∼42″ in ≈1 minute (from 66 to 67 minutes) and, again, lasts for ≈5 minutes with redshift of the plasma. This motion has an apparent velocity of ∼180 km s^{-1}, hence, Alfvénic in nature, perhaps implying that magnetic reconnection may have driven the initially smaller jet to a greater height. The final stage shows some strongly blueshifted plasma as the jet event comes to an end within a further ≈5 minutes. The total duration of this event is ∼15 minutes. Due to the off-limb nature of this event, it is difficult to infer the line-of-sight plasma shift given the uncertainty in the projection angle. Hence, redshifted plasma, may, in fact, represent plasma outflow along an open magnetic field line projected in a direction away from the observer. Given the three stages of this event, it could be interpreted that there are some explosive processes occurring in the initially smaller jet which cause the plasma to accelerate to an even greater height.

When we study marker B (between 67–71 minutes and ≈25–27″ along Solar Y), we find a redshifted wing in the spectral line profile (along with line broadening). After double Gaussian fitting, this wing can be shown to have a Doppler velocity shift in the range of 70–90 km s^{-1}. The radiance of this line emission is substantially greater than the overplotted mean (spatially

averaged) line profile which suggests additional heating of the plasma. When we consider the temporal variation of the line profile in the jet (with marker D), we can find more evidence of line width broadening. This sporadic non-thermal activity, in the course of the jets lifetime, should be identifiable in jets which are observed on-disk and which are projected toward the observer.

3.2. Jet 2

Next, we turn our attention to an on-disk event. The event shown in Figure 5 is very much analogous to Jet 1 with respect to its evolution. In N IV 765 Å, there is increased radiance which coincides with strong FWHM activity at Solar $Y = -149″$, for ≈5″–10″, over a time interval of ≈5 minutes (between 195 minutes and 200 minutes). The temporal variation of the line profiles for this event, as indicated with marker D, shows increasing intensity from 196 minutes until 199 minutes with some non-Gaussian features growing significantly from $t = 197$ to 199 minutes. There is a strong signal to noise given the 30 s exposure time for this observation. The initial jet surge is followed by increased line broadening in the jet. A second event occurs at Solar $Y = -151″$ and at $t = 218$ minutes with similar activity in the FWHM map, although, with no substantial radiance enhancement. It is unclear whether these events are related.

When we inspect the Ne VIII 770 Å line parameter map for this region (as marked by D profiles), we see a strong Doppler
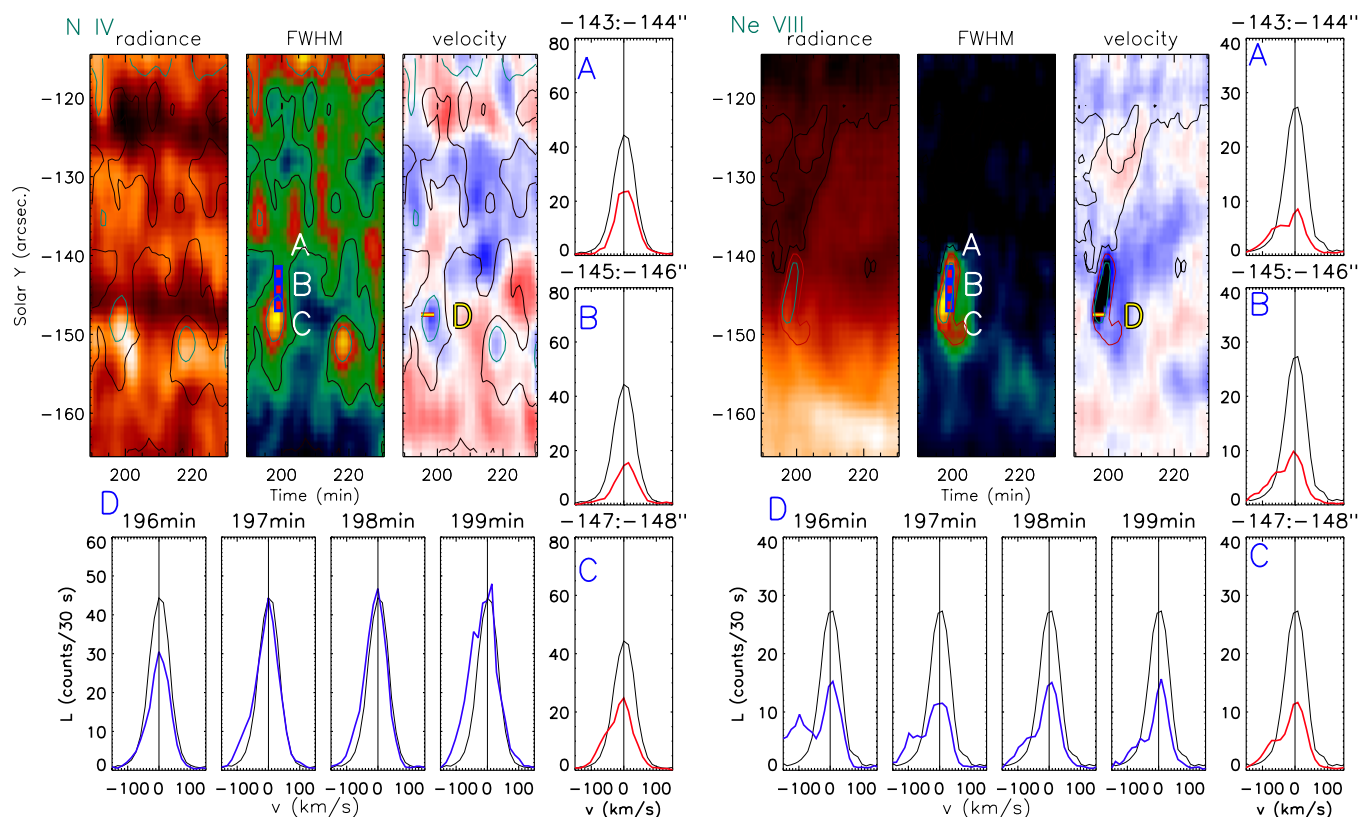
Figure 5. Time-series radiance, Doppler velocity, and width (FWHM) maps in N IV 765 Å (left) and Ne VIII 770 Å (right) for a macrospicule/cool loop event occurring on-disk in the NPCH. The contours on the radiance and Doppler velocity maps, for the N IV 765 Å line, are the contours of the FWHM data with values of 1.6 spectral pixels (light) and 1.8 spectral pixels (dark). The contour (red) on the radiance and Doppler velocity maps, for the Ne VIII 770 Å line, are the contours of the FWHM data with a value of 2.1 spectral pixels. The contour (dark) of the radiance map is plotted onto the FWHM and Doppler velocity maps.

(A color version of this figure is available in the online journal.)

shift in the blue and substantial line broadening along the length of a more extended jet-like structure. From markers A, B, and C, we observe that the line profiles exhibit substantial blue wing formation which corresponds to outflow in the range of 80–100 km s^{-1}. However, when we investigate the line profiles at the source of the jet outflow, we observe even stronger blueshift with a dominant wing formation at $t = 195$ minutes and $t = 196$ minutes.

Figure 6 presents the double Gaussian fitting of the locations marked by D in the Ne VIII 770 Å emission. The blueshifted wing of the emission line is well fitted with a second Gaussian line profile (orange) for the wing component as well as a Gaussian for the line itself (green). The wing component reaches a maximum of 145 km s^{-1} at $t = 195$ minutes and is shown to evolve over the 5 minutes interval with decreasing intensity and velocity. Clearly, FWHM mapping is crucial in the identification process of this event in the hotter line. After 5 minutes, the extent of the line shift declines to 60 km s^{-1}. The stronger signal in Ne VIII 770 Å may indicate that the trigger for this event occurs higher in the solar atmosphere. The activity may then continue downward to the lower atmosphere creating increased activity in N IV 765 Å within the period from $t = 198$–200 minutes.

Another interesting feature is the presence of a cool structure in the Ne VIII 770 Å radiance map. We can identify a long, dark strand extending northward beyond the path of the jet trajectory which is present on the radiance map between $-140''$ and $-120''$ in Solar Y and at $t = 195$–200 minutes. This dark strand is marked with a contour and extends up to $\approx -123''$ in Solar Y until $t = 210$ minutes. This dark strand coincides with a notably redshifted region in the Ne VIII 770 Å Doppler velocity map
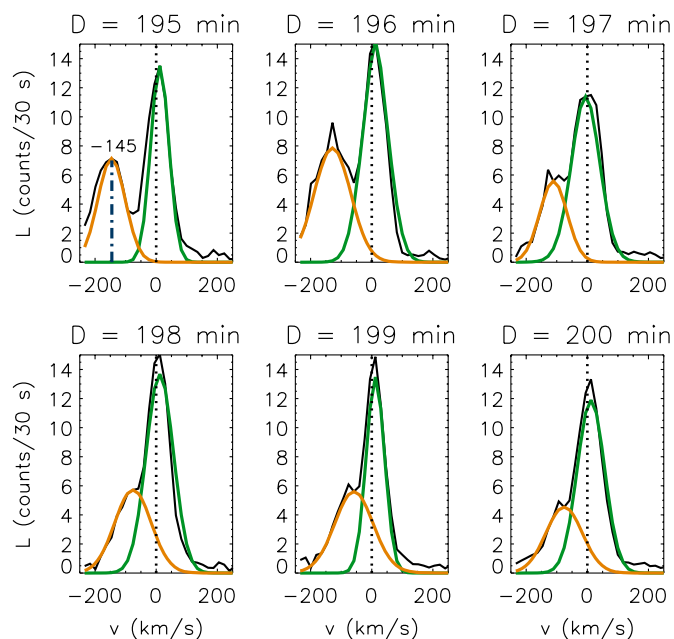
Figure 6. Ne VIII 770 Å spectral line profiles (black) for region D have significantly strong wing formation (main line: green; wing component: orange) which evolve with time from top left to bottom right. Such spectral line profiles are well fitted with double Gaussian line profiles as demonstrated here.

(A color version of this figure is available in the online journal.)

with comparable spatial size and duration as with the source of the jet. In fact, the dark strand in the Ne VIII 770 Å map may
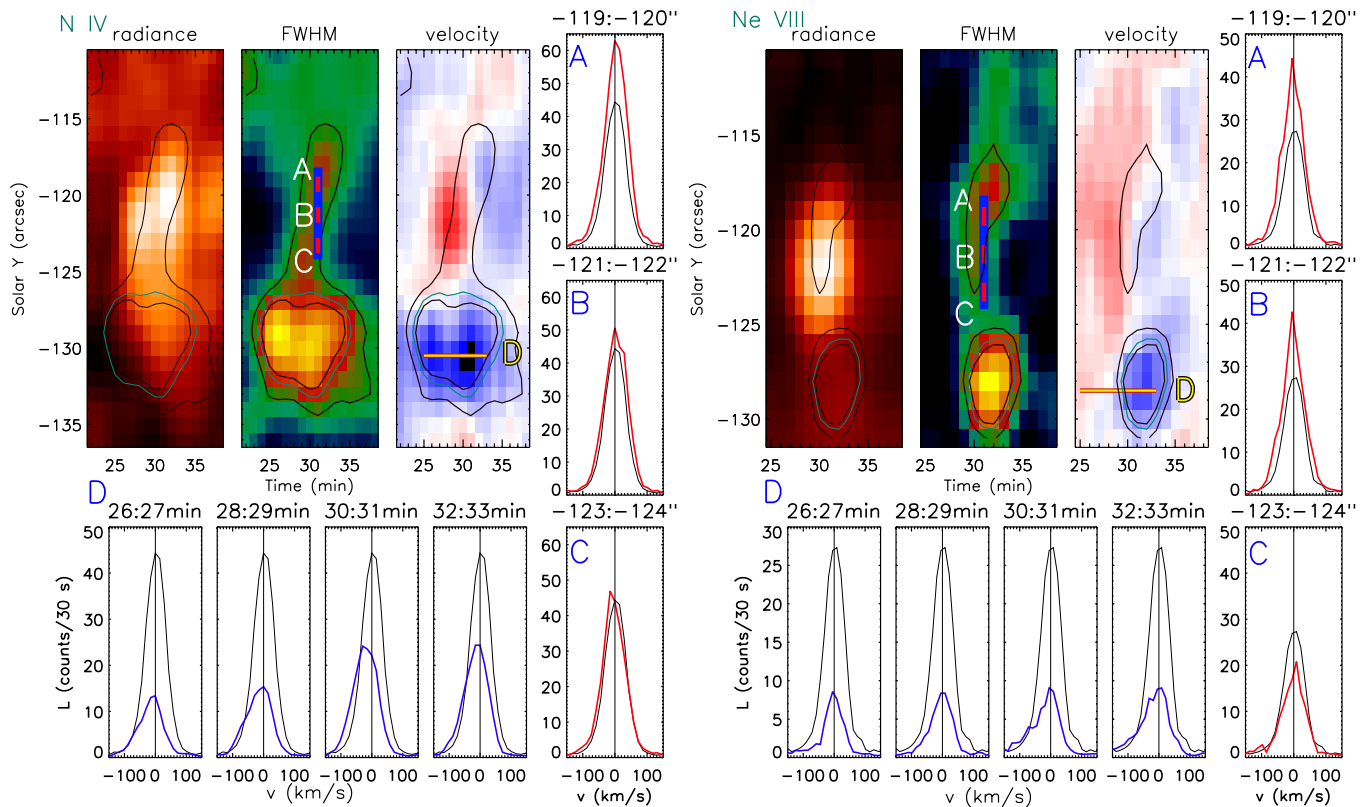
Figure 7. Time-series radiance, Doppler velocity, and width (FWHM) maps in N IV 765 Å (left) and Ne VIII 770 Å (right) for a macrospicule/hot loop/blinker event that occurred on-disk in the NPCH. The contours on the radiance and Doppler velocity maps, for both lines, are the contours of the FWHM data with values of 1.8 spectral pixels (light) and 2.0 spectral pixels (dark). Hence, the extent of line shifting for this event is comparable to Jet 2 but greater than for Jet 1.

(A color version of this figure is available in the online journal.)

indicate the presence of cool plasma in a hot environment. The outflow through the dark strand lasts for an interval of 5 minutes followed by a 3 minute interval of net zero line shift and, finally, a subsequent 5 minute interval of redshift. We could interpret that the plasma flows through the dark strand and sourced from the strongly blueshifted jet. This event will be discussed further in the discussion section in the context of a cool loop formation.

3.3. Jet 3

In the N IV 765 Å line (see Figure 7), we observe substantial line broadening between $-127''$ and $-133''$ on Solar Y which commences at $t = 25$ minutes and lasts for 10 minutes. The spectral line profiles marked by D show the Ne VIII 770 Å line variation throughout this event. This region shows increasing line broadening and radiance with time (as compared with Jet 1) plus a blue wing. We see two consecutive blueshifted regions implying repetitive jet formation over the 10 minutes event interval. The second jet, lasting for 5 minutes, appears to have the strongest blueshifted velocities greater than 15 km s^{-1} as opposed to the first jet (also 5 minutes duration) which has a velocity in the blue of $\approx$10 km s^{-1}. The spatial coverage of the blueshifted region along the slit is spicule like ($\sim$3$''$).

Another major feature of this event is the poleward projection of the line width broadening from the point of ejection of the first jet. The top side of this extension in the FWHM map occurs between $-118''$ and $-119''$ on Solar Y. This extension, in the FWHM map, is contoured and overplotted in the Doppler velocity map and corresponds well with the first jet blueshift followed 2–3 minutes later with strong redshifting in the plasma. The extension in the FWHM map from the center of the first

jet ($-130''$ in Solar Y) to the center of the redshifted region ($-121''$) could indicate the presence of a closed magnetic loop which connects the two regions. Alternatively, the red-to-blue line shifting on-disk with increased line broadening, as presented in the upper section of the line maps, has been previously interpreted as rotational plasma motion in an on-disk macrospicule event. Rotating features in transition region lines were reported by Pike & Mason (1998) and Banerjee et al. (2000).

Evidence for explosive activity in N IV 765 Å could be interpreted 3–5 minutes after the first blueshift event (in the lower region of the Doppler velocity maps) as the development of a stronger blueshift which demonstrates increased radiance and more evident line width broadening (see D). When we consider the Doppler velocity map of this jet formation in Ne VIII 770 Å, we find that there is no evidence of the first jet event. There is no blueshift of the plasma between $t = 25$ minutes and $t = 30$ minutes, whereas, the second stronger blueshifting (from N IV 765 Å Doppler velocity map) is the only feature to become visible in the Ne VIII 770 Å Doppler velocity map.

One might interpret this event as a series of two jet events (whereby the first jet drives the larger second jet as for Jet 1) or perhaps flows along a hot loop connecting the events in the lower and upper sections of the map. To investigate this further, Figure 8 plots data cross-cuts of the Doppler velocity (black line) and radiance (blue line) temporal variations of both N IV 765 Å (solid) and Ne VIII 770 Å (dashed). At location B along the slit, there is an obvious red- to blueshift of the plasma from 19 km s^{-1} to -10 km s^{-1} in N IV 765 Å for 8 minutes and, likewise, from 12 km s^{-1} to -5 km s^{-1} in Ne VIII 770 Å for 3–4 minutes. The blueshift in Ne VIII 770 Å occurs 1 minute before
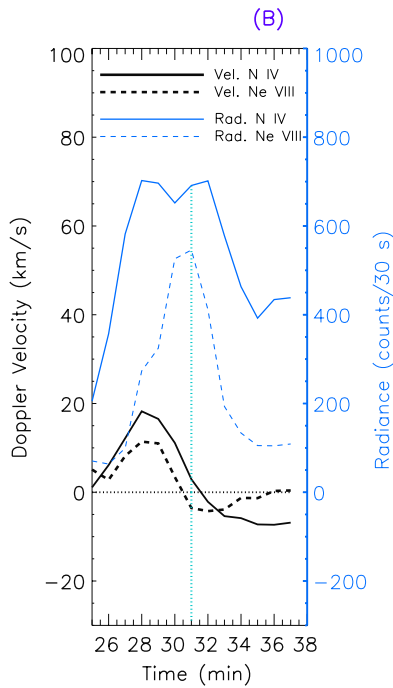
Figure 8. Radiance (blue) and velocity (black) variations for N IV 765 Å (solid) and Ne VIII 770 Å (dashed) at marker B (see the legend). The left-hand y-axis of each plot is scaled for the Doppler velocity measurement in time. The right-hand y-axis of each plot is scaled for the radiance measurements in time. We note that red-to-blue plasma shifts correspond to sharp increases in the radiance intensity of both lines with respect to the event presented in Figure 7.

(A color version of this figure is available in the online journal.)

the blueshift in N IV 765 Å. The line shift coincides with a sharp increase in the radiance profile of Ne VIII 770 Å to a peak of 550 counts/30 s. There are multiple increases in the radiance profile for N IV 765 Å and both peaks are stronger than the single peak of Ne VIII 770 Å (650 counts/30 s lasting 4–5 minutes). Notably, the first radiance peak in N IV occurs before the Ne VIII peak.

However, what is important here is the delay in the response of the two lines. Given that the strongest component of the plasma outflow and the strongest radiance component exist in the N IV 765 Å, therefore, the mechanism driving the outflow may occur in the lower atmosphere. Hence, any effects on the plasma should appear in the hotter line only after appearing in the cooler line. The multiple "flashes" of intensity in N IV 765 Å, separated by 4 minutes, may be the signature of repeated reconnection given that there is significant line broadening in the spectral profile of marker B.

3.4. Jet 4

Figure 9 presents an off-limb macrospicule event for the SPCH data set. In comparison with the result presented for the NPCH off-limb macrospicule, this event is more clearly resolved in N IV 765 Å than in Ne VIII 770 Å. It has a distinct three-stage morphology which describes a small blueshifted jet (between $t = 762$ minutes and $t = 768$ minutes) preceding a dominant red-to blueshift in the more extended second jet lasting $\approx$19 minutes after the rise of the first jet (between $t = 769$ minutes and $t = 788$ minutes). Also, the maximum height above the limb of the second stage is 40″. However, in this event the larger jet has a much more dominant redshift component (lasting $\sim$11 minutes) than in Jet 1 (which lasts for $\approx$2–3 minutes) which could result in a longer overall event duration ($\approx$10 minutes longer).

The fast rise of the initially smaller jet from a height of 25″ at $t = 764$ minutes to a maximum height of 40″ in the second stage within 9 minutes implies a rise velocity of $\sim$20 km s^{-1}. This increased duration in the acceleration stage of the event, including the redshift region, implies a larger jet event, although, this has not resulted in a more extended jet off-limb compared with Jet 1. In the line profile variation of marker D, we observe a dominant redshift of the N IV 765 Å line with a strong wing at $t = 770$ minutes which can be fitted with a double Gaussian. Its wing component has a velocity of 50–100 km s^{-1}. The extent of this red wing formation declines at $t = 771$ minutes and is no longer present at $t = 772$ minutes. Hence, an explosive event occurs between 769 and 770 minutes at $\approx -13''$ accelerating the plasma present in the earlier smaller jet from $\approx$25″ to 40″ off-limb with continued redshift (10–15 km s^{-1}) until finally evolving into a lesser blueshifted component.

The key to understanding the implications of these differences (when compared with Jet 1) may be found in the observed line width broadening activity in Ne VIII 770 Å. We observed a distinct increase in the Ne VIII 770 Å line width broadening extending from the limb to 40″ over an interval ($\sim$11 minutes) between $t = 765$ minutes and $t = 776$ minutes. The line profiles for marker D (furthest off-limb) show significant broadening at $\approx 14''$–15″ off-limb with increased radiance compared with the mean spectral line profile (black). At 772 minutes, the radiance of the line emission is $\approx$6 times greater than the mean line profile. Line broadening is evident in the profiles marked by A, B, and C between 6″ and 13″ off-limb. This activity in Ne VIII 770 Å is not so obvious in the radiance map (unlike in the radiance map of N IV 765 Å) but what is clear is that this event is strongly observed in the line width map. This observation leads us to believe that some heating may occur in the lower corona, unlike with Jet 1.

4. DISCUSSION

Analysis of the data for the studied NPCH and SPCH has revealed jet-like features both off-limb and on-disk with distinct and comparable features which may enable us to further understand the evolution of these dynamic events. The features that reveal cool spicular events, commonly seen off-limb in the contrast of a dark background, can be made identifiable on-disk. Next, we will discuss the nature of the jets described in Section 3 along with the other components which may be associated with their formation.

4.1. Jets On-disk and Off-limb

The observation presented in Figure 4 shows a dynamic event in a coronal hole that reaches apparent rise velocities of $\sim$180 km s^{-1} in the cooler N IV 765 Å line. The feature extends from the solar limb in N IV 765 Å to 40″ in 10–15 minutes which is typical of macrospicule morphology. The three-stage morphology of the jet seen off-limb in Figure 4 is remarkably similar to the off-limb event seen in Figure 9. The NPCH data set from Figure 2 revealed periodic plasma outflows which precede the events described in Jet 2. This on-disk activity in N IV 765 Å, with coinciding activity in Ne VIII 770 Å, is somewhat similar to transition region explosive events (TREEs). TREEs were recently observed to occur in bursts with a period of 3–5 minutes as a result of either kink mode oscillations in closed loops undergoing reconnection (Doyle et al. 2006), or by propagating p-mode oscillations into the upper chromosphere (De Pontieu et al. 2004; De Pontieu & Erdélyi 2006; Chen &
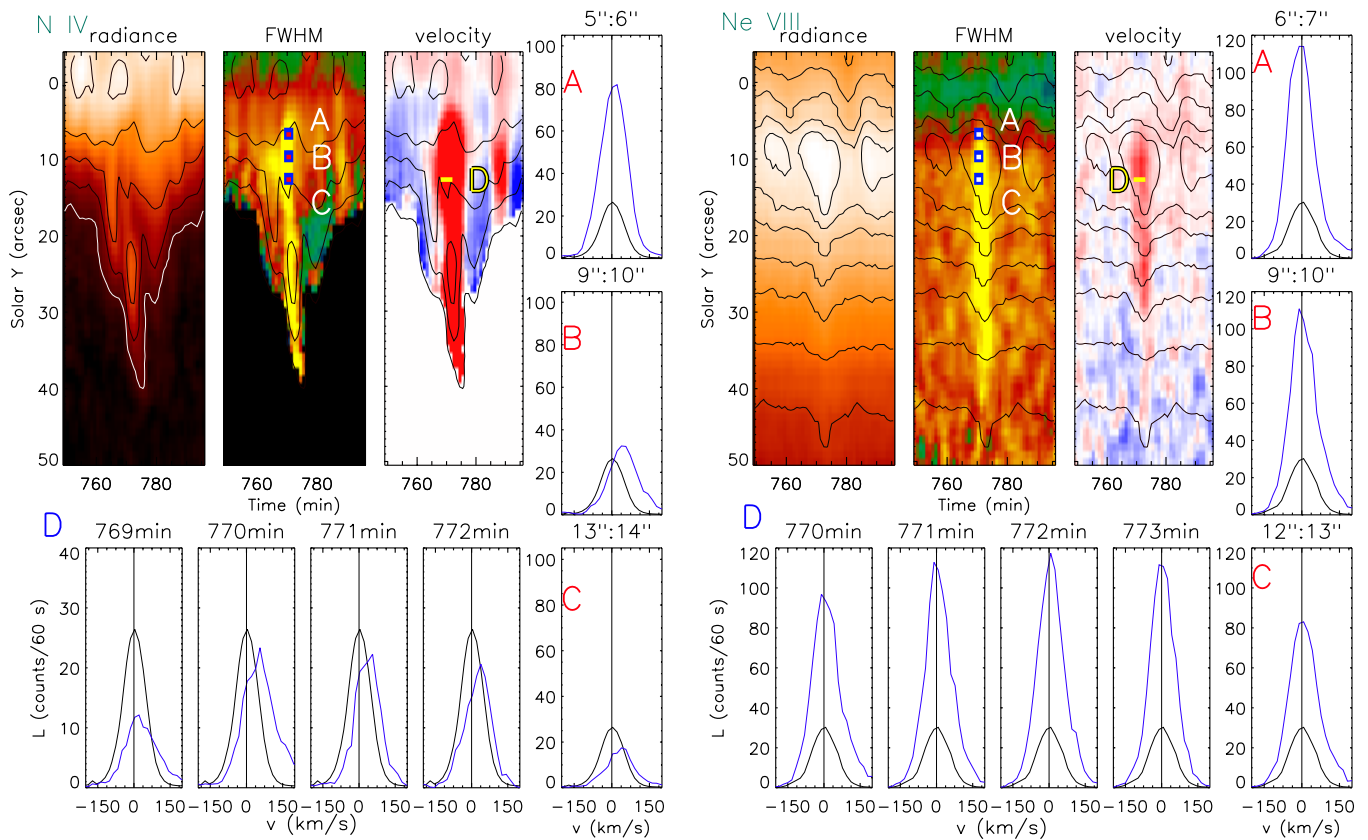
Figure 9. Time-series radiance, Doppler velocity, and width (FWHM) maps in N IV 765 Å (left) and Ne VIII 770 Å (right) for a macrospicule event occurring off-limb in the SPCH. Surrounding each of the line parameter maps are the fitted spectral line profiles representing the locations marked on the maps by A, B, and C (red spectral profiles) which describe the spatial evolution of the line at one time. Marker D (blue spectral profiles) describes the temporal evolution of the line at one location along the slit. The black line profile represents the mean line profile found through summing all fitted spectral pixel windows on-disk for the full duration of the observation. The contours on the FWHM and Doppler velocity maps, for both lines, are the contours of the radiance data highlighting strong intensity regions in the duration of the event (dark).

(A color version of this figure is available in the online journal.)

Priest 2006). Recent data analyzed by Doyle et al. (2006) suggest two types of TREEs—one formed in the low chromosphere and the other in the mid-to-high TR. Zaqarashvili et al. (2007) found that through measuring the relative Fourier phase between oscillations of spicules at different heights the most pronounced periods at both heights are 180 and 30 s. As a result, there maybe a connection between spicule activity and TREEs formed in the mid-to-high TR. In our results, we presented evidence of similar activity but with a longer burst periodicity of ∼20–25 minutes. To interpret this activity, Gupta et al. (2009) detected the presence of waves from the same NPCH data set used in this study through measuring the phase delays between intensity oscillations as well as between velocity oscillations. In doing so, they were able to measure the travel time of the propagating oscillations and ultimately the propagation speeds of the waves that produce the oscillations. The NPCH data set reveals long period compressional waves with a dominant period of ∼25 minutes which are subsonic in nature. In conclusion, we can state that the 20–25 minute blueshifted bursts preceding the on-disk Jet 2 event may be driven by subsonic pulsations. If so, these repetitive bursts would be spicule-like, i.e. wave-driven outflows on-disk, but differ, such that they have a significantly larger spatial coverage (25″).

Banerjee et al. (2009) carried out a joint observing study of pCHs to investigate the role of waves in the acceleration of the fast solar wind with SUMER and the EIS spectrometer. Through analysis of Ne VIII 770 Å along with the hotter EIS

Fe XII 195 Å ($T = 1.3$ MK) line, they also detected long period oscillations with periods of 10–30 minutes. The presence of outward propagating waves in the lower atmosphere of pCHs may play a role in driving the plasma jets to greater Doppler blueshifts and line widths in the outer atmosphere, as outlined in Jet 2. The maximum Doppler velocity for Jet 2 is greater in the hotter line than in the cooler line despite the fact that the blueshift of the event first appears in the cooler line. Zaqarashvili et al. (2007) found that the maximum Doppler velocity increases in consecutive height series for spicule-like jets.

Anomalous resistivity could become important in driving magnetic reconnection as a result of the initial jet propagation (Chen & Priest 2006). In other words, an initially smaller wave-driven jet may trigger reconnection between the open and closed magnetic fields and so the smaller jet evolves into a larger jet with a component of the plasma traveling through the cool loop. This description could be applicable to all jets discussed here.

With high spatial and temporal resolution, we are capable of revealing that localized heating does occur in some jets/macrospicules with evidence from Jet 4 showing increased line width broadening in Ne VIII 770 Å. The fact that the event is more extended in time (almost twice as long compared to a similar event in Jet 1) than in space (same rise height of the second jet off-limb) may mean that more energy was deposited in the upper atmosphere in heating (making it visible in Ne VIII 770 Å) rather than being converted to kinetic energy to drive the

plasma further off-limb. Doyle et al. (2005) suggested that the increase in line broadening off-limb may not be due to small-scale random motions but rather a superposition of line shifts due to spicules and/or macrospicule activity. Line broadening is, indeed, evident with our observations of macrospicules from both NPCH and SPCH off-limb particularly in localized regions in the FWHM maps. There exist subtle differences between Jets 1 and 4 with respect to the overall duration and the greater redshift phase of the macrospicule event in Jet 4. The key difference is the presence of Ne VIII 770 Å in one of the jets. This leads us to conclude that both jets are driven by the same physical mechanism, e.g., magnetic reconnection given the explosive nature of the plasma. An important consequence of their subtle differences leads to energy release, as in Jet 4, which is transferred into heating of the upper atmosphere. We find that the differences between macrospicule Jet 1 and Jet 4 show remarkably strong similarities in comparison with the differences between Type-I and Type-II spicules. The notable differences between Type-I and Type-II spicules are the increased jet lifetime with reduced rise velocity (non-Alfvénic in nature) for Type I over Type II. Likewise, macrospicule Jet 4 has an increased lifetime and non-Alfvén rise velocity ($\sim$20 km s^{-1}) compared with Jet 1 ($\sim$180 km s^{-1}). Yet the two events are almost identical spectroscopically with respect to their morphology, as discovered via Doppler velocity mapping. As discussed, our spectroscopic study of Jet 4 potentially reveals atmospheric heating given increased line width measurements in the hotter Ne VIII 770 Å line upon the rise of the jet which was otherwise non-existent in Jet 1. It may be interesting to determine whether a similar spectroscopic signature in the hotter lines exist for Type-I spicules in comparison with Type II. This approach could allow us to draw more information regarding the heating implications of spicules in the lower solar atmosphere and the extent to which Type-I and Type-II spicules contribute to the fast solar wind.

Langangen et al. (2008) presented a disk counterpart of Type-II spicules which they named as rapid blueshift events (RBEs). RBEs have typical lifetimes of Type-II spicules but at reduced heights and lower rise velocities. Langangen et al. (2008) concluded, via Monte Carlo simulations, that the reason for the lower velocity RBEs was a result of the inverse relationship between the density and velocity of the events. High-density and low-velocity events show enough absorption to be visible on-disk, whereas low-density high-velocity events are more clearly visible off-limb but have little visibility on-disk due to their low opacity. With this idea in mind, we could add more weight to the argument that macrospicule Jet 1 is characteristic of a Type-II spicule when compared with Jet 4 (Type I). Jet 1 is faint in N IV 765 Å and non-existent in Ne VIII 770 Å emission and has the highest measured rise velocity, therefore, is typical of Type-II spicules off-limb with low densities. In this case, Jet 2 would resemble an RBE but on a macrospicule spatial scale given its weaker, yet substantial, blueshifting of the material in Ne VIII 770 Å. Based on this evaluation, it may be true that macrospicules observed on-disk with lower blueshifted velocities, which resemble RBEs on a larger spatial scale, are driven by magnetic reconnection in the lower and denser atmosphere. Whereas, faster and less dense macrospicule events (more easily seen off-limb as for Jets 1 and 4) are driven by magnetic reconnection which is triggered further upward in the mid to lower corona.

Recently, McIntosh & De Pontieu (2009) explored a joint observation of the southeast limb with *Hinode*/SOT Ca II H,

Transition Region and Coronal Explorer (*TRACE*) 1600 Å, and SUMER (lines Ne VIII 770 Å, N IV 764 Å, and O VI 786 Å). A macrospicule was observed and crossed the line of sight of the SUMER detector B slit. Space–time analysis with SOT and *TRACE* revealed with jet-ejected material which followed a parabolic trajectory (characteristic of Type-I spicules) with velocity of $\sim$40 km s^{-1} measured after 7 minutes. This jet was described as being similar to a Type-I spicule event though with larger spatial coverage. As discussed, we draw similar conclusions for Jet 4. Although we reveal new heating implications with regards to macrospicules with a longer lasting redshift phase. Furthermore, we find that the repetitive bursts of plasma observed on-disk which commence up to 80 minutes prior to Jet 2, also, indicate this activity. Unlike McIntosh & De Pontieu (2009), we detect strong emission in Ne VIII 770 Å for Jet 5 as the ejected material enters a redshift phase. McIntosh & De Pontieu (2009) suggest that a lack of emission in Ne VIII is due to the material becoming a constituent of the corona. We find that there can exist macrospicule structures which have no Ne VIII 770 Å emission (Jet 1) but, also, those that do (Jet 4). We also find that those which exhibit no Ne VIII 770 Å emission can have larger rise velocities (Alfvénic in nature), implying turbulent and energetic plasma, than those that do. Maybe macrospicules like Jet 1 are becoming ejected completely and forming the fast component of the solar wind rather than becoming constituents of the corona and heating the outer atmosphere (which is possibly happening in Jet 4). Baker et al. (2008) analyzed EIS and XRT observations of hot jets in coronal holes on-disk in multiple wavelengths. They observed a jet with a postjet increase in its EUV light curve. They suggested that this feature arises because the hot plasma, having failed to reach escape speeds, cools and falls back. They concluded that the fall-back of plasma provided some evidence of impact heating. We agree that the largely redshifted plasma of Jet 4 (with substantially smaller apparent rise velocity compared with Jet 1), along with additional line broadening in Ne VIII, may provide some evidence of atmospheric heating. We need to address more specifically how the ejected material from a macrospicule can become a constituent of the corona and under what circumstances will it become completely ejected and/or fall back. Further statistical analysis of both on-disk and off-limb examples of macrospicule jets in pCH, via spectrscopic approach, is required.

We can draw further conclusions on the similarities between macrospicules observed on-disk and those off-limb. Macrospicules could be observed on-disk with a loop extending away from the jet, as discussed for Jet 3, with magnetic reconnection between open fields and erupting loops in the mid-solar atmosphere. This scenario was presented in a blinker model by Doyle et al. (2004). The hot loop event of Jet 3 could be interpreted as a blinker when observing the Ne VIII 770 Å line emission. Given this comparison, we can connect the spicules to macrospicules observationally and, also, macrospicules to blinkers. These results are in agreement with findings by Madjarska et al. (2007).

4.2. Cool Loop Event

Given the huge velocity outflow in Ne VIII 770 Å in Jet 2 (145 km s^{-1}), we expect that this on-disk event is more energetic than the off-limb macrospicule due to substantial heating allowing the jet to be observed in Ne VIII 770 Å. This is an example of how much priority needs to be given to the line profiles structure before assigning a line-of-sight Doppler velocity measurement

of a strongly blueshifted region. Global FWHM mapping is a good indicator of where wing formation is occurring in the full data set of line profiles, hence, identifying more effectively where significant plasma outflow occurs.

The formation mechanism for Jet 2 is most likely magnetic reconnection of the photospheric magnetic field on the supergranular scale. This determination is in agreement with the results of similar structures observed by McIntosh & De Pontieu (2009). The magnetic reconnection is triggered and the re-configuration of the magnetic topology results in continued explosive activity downward along the newly formed current sheet. The downward propagation of this explosive activity is evident in the decline of the line width broadening, with time, for the region marked D in Ne VIII 770 Å which coincides with an increase in activity in the N IV 765 Å line for the same region. We have shown in the FWHM map for Ne VIII 770 Å in Jet 2 that the increased line width for the macrospicule-like event lasts for ∼11 minutes and this coincides with redshifting. De Pontieu et al. (2007a) suggested that very long lived macrospicules show evidence of Alfvén waves with periods between 300 and 600 s. They also showed evidence for upward and downward propagating waves in spicule-like events with an estimated phase speed in the range of 50–200 km s^{-1}. Zaqarashvili et al. (2007) estimated the propagation speeds of spicule-like jets as ∼110 km s^{-1}. We estimated a blueshift Doppler velocity for the on-disk event to be ∼145 km s^{-1} which is in agreement with these previous findings as discussed, but in this case, for an on-disk macrospicule-like event associated with a cool loop. We expect that the dark strand observed in Jet 2 reveals the presence of a cool loop with two footpoints which are identified by the blue followed by redshifted plasma. Cool upflows have been identified from EIS (He II and O IV emission) and SUMER (Ne VIII) data which occur in network regions harboring low-lying fields in the transition region (Kamio et al. 2009). They suggested that these flows are produced by an acceleration of plasma in the chromosphere which propagate into the transition region. It is proposed that the cool plasma flow is driven by the magnetic tension force and pressure of reconnected fields and the reconnection accelerates the faster jet component of the event. Kamio et al. (2009) infer that low-lying fields can lead to reconnection in the transition region which results in cool upflows or explosive events and the lack of a coronal counterpart is due to a closed field configuration. A schematic picture of the configuration of this process (which strongly agrees with our observation of Jet 2) is presented in Kamio et al. (2009, Figure 10). Yokoyama & Shibata (1995) previously showed that a cool jet is formed alongside a hot jet. The cool loop may play an important role through driving the magnetic reconnection to aid the macrospicule formation in Jet 2. Could the hotter signatures observed on-disk in Jet 3 indicate hot flow along closed loops, analogous to the cool loop formation discussed? We can use observations, such as for Jets 2 and 3, to constrain our models in predicting cool loops.

We have considered the jet phenomena spectroscopically for both on-disk and off-limb events. The jet morphology appears in stages with periods of small jet outflows followed by large jet outflows coinciding with localized regions of significant line broadening. However, with on-disk observations of jets, we are able to investigate the direction of propagation of the explosive activity in time as seen in Jet 2. It is clear that macrospicules off-limb can be identified on-disk and that an aerial plus side-on perspective of these dynamical structures reveals matching spectroscopic signatures.

5. SUMMARY

In this paper, we found high-velocity features observed simultaneously in spectral lines formed in the mid-transition region (N IV 765 Å) and in the low corona (Ne VIII 770 Å) for both on-disk and off-limb transient and explosive events.

The most interesting finding of this study is the presence of non-Gaussian line profiles showing line-of-sight upflows of ≈80 km s^{-1} not only in the cold N IV 765 Å line on disk in Jet 2 but, also, in the hot Ne VIII 770 Å line where the reported flow speeds become even higher (≈145 km s^{-1}).

We found a number of other interesting events which have similar driving mechanisms but with different consequences and heating effects in the upper atmosphere, i.e., the hot loop and cool loop events. The connection between the on-disk and off-limb events requires further study as we can reveal a direct comparison between stronger macrospicule off-limb (Jet 4) events and hot loop/blinker events on-disk (Jet 3). This same idea applies to the radiantly weaker off-limb macrospicule (Jet 1) comparison with the cool loop/feature which is undetected spectroscopically in coronal holes until now (Jet 2). The on-disk versus off-limb analysis in two emission lines allows for a unique opportunity to study the same event, in a coronal hole, from a side and aerial perspective.

We found that FWHM mapping can reveal many more on-disk jet events than with imaging and Doppler velocity mapping alone. The FWHM parameter is important in the context of how it allows us to identify on-disk jets and explosive events. An accurate determination of the FWHM line parameter for any observation is controlled by the spectral resolution of the instrument used. We find that the SUMER spectrometer is unmatched with respect to its high spectral resolution capability.

We have found that there are a number of important questions which need to be answered from a theoretical perspective. We have shown that spicules can become identifiable on-disk, spectroscopically, as localized plasma outflows in not just the lower solar atmosphere but, also, in the mid-transition region. The events which we have outlined reveal that spicule activity could act as a precursor to macrospicule formation. Thus, do spicules become macrospicules in the event of a (non-)repeating magnetic reconnection as with TREEs? If so, what is the most likely mechanism driving such magnetic reconnection?

Finally, this study highlights the fact that we can advance our understanding of the small-scale structures in the solar atmosphere in the context of how they contribute to two of the big unanswered questions in solar physics: coronal heating and solar wind origin and acceleration. To do so, we need a high-resolution EUV spectrograph (ideally combining a narrowband EUV imaging telescope plus optical data including magnetograms) that should have more improved temporal and spectral resolution in the lower corona and transition region emission lines.

REFERENCES

Baker, D., van Driel-Gesztelyi, L., Kamio, S., Culhane, J. L., Harra, L. K., Sun, J., Young, P. R., & Matthews, S. A. 2008, in ASP Conf. Ser. 397, First Results from *Hinode*, ed. S. A. Matthews, J. M. Davis, & L. K. Harra (San Francisco, CA: ASP), 23
Banerjee, D., O'Shea, E., & Doyle, J. G. 2000, A&A, 355, 1152
Banerjee, D., Teriaca, L., Gupta, G. R., Imada, S., Stenborg, G., & Solanki, S. K. 2009, A&A, 499, L29
Beckers, J. M. 1972, ARA&A, 10, 73
Chen, P. F., & Priest, E. R. 2006, Sol. Phys., 238, 313
Chifor, C., et al. 2008, A&A, 491, 279
Cirtain, J. W., et al. 2007, Science, 318, 1588
Culhane, J. L., et al. 2007, Sol. Phys., 243, 19
Dammasch, I. E., Wilhelm, K., Curdt, W., & Hassler, D. M. 1999, A&A, 346, 285
De Pontieu, B., & Erdélyi, R. 2006, Phil. Trans. R. Soc. A, 364, 383
De Pontieu, B., Erdélyi, R., & James, S. P. 2004, Nature, 430, 536
De Pontieu, B., Hansteen, V. H., Rouppe van der Voort, L., van Noort, M., & Carlsson, M. 2007a, ApJ, 655, 624
De Pontieu, B., et al. 2007b, Science, 318, 1574
De Pontieu, B., et al. 2007c, PASJ, 59, 655
Doschek, G. A., et al. 2007, ApJ, 667, L109
Doyle, J. G., Giannikakis, J., Xia, L. D., & Madjarska, M. S. 2005, A&A, 431, L17
Doyle, J. G., Popescu, M. D., & Taroyan, Y. 2006, A&A, 446, 327
Doyle, J. G., Roussev, I. I., & Madjarska, M. S. 2004, A&A, 418, L9
Golub, L., et al. 2007, Sol. Phys., 243, 63
Gupta, G. R., O'Shea, E., Banerjee, D., Popescu, M., & Doyle, J. G. 2009, in Astrophysics and Space Science Proc., Magnetic Coupling between the Interior and the Atmosphere of the Sun, ed. S. S. Hasan & R. J. Rutten (Berlin: Springer)
Jess, D. B., Mathioudakis, M., Erdélyi, R., Crockett, P. J., Keenan, F. P., & Christian, D. J. 2009, Science, 323, 1582
Kamio, S., Hara, H., Watanabe, T., & Curdt, W. 2009, A&A, 502, 345
Kamio, S., Hara, H., Watanabe, T., Matsuzaki, K., Shibata, K., Culhane, L., & Warren, H. P. 2007, PASJ, 59, 757
Kosugi, T., et al. 2007, Sol. Phys., 243, 3
Krieger, A. S., Timothy, A. F., & Roelof, E. C. 1973, Sol. Phys., 29, 505
Langangen, Ø., De Pontieu, B., Carlsson, M., Hansteen, V. H., Cauzzi, G., & Reardon, K. 2008, ApJ, 679, L167
Moreno-Insertis, F., Galsgaard, K., & Ugarte-Urra, I. 2008, ApJ, 673, L211
Madjarska, M. S., Doyle, J. G., Innes, D. E., & Curdt, W. 2007, ApJ, 670, L57
McIntosh, S. W., & De Pontieu, B. 2009, in Proc. Second *Hinode* Science Meeting, in press (arXiv:0901.2814)
Munro, R. H., & Withbroe, G. L. 1972, ApJ, 176, 511
Nishizuka, N., Asai, A., Takasaki, H., Kurokawa, H., & Shibata, K. 2009, ApJ, 694, L74
Patsourakos, S., Pariat, E., Vourlidas, A., Antiochos, S. K., & Wuelser, J. P. 2008, ApJ, 680, L73
Pike, C. D., & Mason, H. E. 1998, Sol. Phys., 182, 333
Popescu, M. D., Banerjee, D., O'Shea, E., Doyle, J. G., & Xia, L. D. 2005, A&A, 442, 1087
Popescu, M. D., Xia, L. D., Banerjee, D., & Doyle, J. G. 2007, Adv. Space Res., 40, 1021
Savcheva, A., et al. 2007, PASJ, 59, 771
Shibata, K., Nozawa, S., & Matsumoto, R. 1992, PASJ, 44, 265
Sterling, A. C. 2000, Sol. Phys., 196, 79
Suematsu, Y., Ichimoto, K., Katsukawa, Y., Shimizu, T., Okamoto, T., Tsuneta, S., Tarbell, T., & Shine, R. A. 2008, in ASP Conf. Ser. 397, First Results from *Hinode*, ed. S. A. Matthews, J. M. Davis, & L. K. Harra (San Francisco, CA: ASP), 27
Tsuneta, S., et al. 2008, Sol. Phys., 249, 167
Wilhelm, K., et al. 1995, Sol. Phys., 162, 189
Xia, L. D. 2003, PhD thesis, Georg-August-Univ., Göttingen
Yokoyama, T., & Shibata, K. 1995, Nature, 375, 42
Zaqarashvili, T. V., & Erdélyi, R. 2009, Space Sci. Rev., in press (arXiv:0906.1783)
Zaqarashvili, T. V., Khutsishvili, E., Kukhianidze, V., & Ramishvili, G. 2007, A&A, 474, 627
Zaqarashvili, T. V., & Skhirtladze, N. 2008, ApJ, 683, L91